Journal of Neuroimmune Pharmacology (2019) 14:709–719
https://doi.org/10.1007/s11481-019-09872-z

ORIGINAL ARTICLE

Low-Dose Subcutaneous Anti-CD20 Treatment Depletes Disease Relevant B Cell Subsets and Attenuates Neuroinflammation

Catherine Huck[1] · David Leppert[2] · Vanessa Wegert[1] · Cindy Schmid[1] · Robert Dunn[3] · Gisbert Weckbecker[1] · Paul A. Smith[1]

Received: 11 July 2019 / Accepted: 1 August 2019 / Published online: 21 August 2019

Abstract

To explore the B cell depleting capacity of a low-dose (20 μg) subcutaneous mouse anti-CD20 antibody treatment on disease-relevant B cell populations within lymph nodes and the spleen. B cell depleting capacity was explored in healthy female C57BL/6 and BALB/c mice; following immune activation in two different mouse models: trinitrophenylated lipopolysaccharide model (thymus-independent response) and dinitrophenyl-keyhole limpet hemocyanin model (thymus-dependent response); and in a chronic neuroinflammation experimental autoimmune encephalomyelitis model. CD20 protein expression on B cell subpopulations was also studied. The subcutaneous anti-CD20 regimen resulted in rapid depletion of B cells in blood, lymph nodes and spleen. Low-dose subcutaneous treatment did not reduce antigen-specific immunoglobulin M and immunoglobulin G titers in all subgroups, and relatively spared splenic marginal zone (MZ) B cells in both T cell dependent and T cell independent B cell immunization models. Analysis of immune compartments during anti-CD20-modulated autoimmune neuroinflammation showed that the maximal B cell depletion was achieved within 2 days of treatment and was highest in the lymph node. Regardless of the tissues analyzed, low-dose subcutaneous treatment was characterized by rapid B cell repletion following treatment cessation. CD20 protein expression was consistent on all B cell subsets in blood, and was more pronounced in germinal center B cells of lymph nodes and MZ B-cells of the spleen. Low-dose subcutaneous anti-CD20 therapy effectively depleted B cells within lymphatic tissues and reduced the severity of neuroinflammation. These data suggest that subcutaneous anti-CD20 therapies can effectively target disease-relevant B cell populations, have shorter repletion kinetics and maintain vaccination responses, thereby achieving autoimmune amelioration without severely impacting immune surveillance functions.

Keywords Subcutaneous · Anti-CD20 monoclonal antibody · Ofatumumab · Marginal zone B cells · Lymph node · Spleen

Introduction

Anti-CD20 monoclonal antibody (mAb)-mediated B cell depletion therapies have contributed to our understanding of the role of B cells in several autoimmune diseases. In recent years, these therapies have become a cornerstone for the treatment of autoimmune diseases such as rheumatoid arthritis and multiple sclerosis (MS) (Bar-Or et al. 2018; Gong et al. 2005; Gorman et al. 2003). MS is a chronic inflammatory demyelinating disease of the central nervous system (Lemus et al. 2018). Rituximab, a murine-human chimera, was the first anti-CD20 antibody to be tested in MS trials which led to the development of ocrelizumab (the humanized successor of rituximab) and fully human ofatumumab (Bar-Or et al. 2008; Du et al. 2017; Hauser et al. 2008). Ocrelizumab has been approved for relapsing-remitting MS, while ofatumumab is being investigated in Phase 3 trials in patients with MS (Mulero et al. 2018). Ofatumumab, administered at low-dose subcutaneously (s.c.), showed potent suppression of clinical signs of MS in the MIRROR study (Bar-Or et al. 2018). It exhibits unique binding to a composite epitope of CD20 close

Electronic supplementary material The online version of this article (https://doi.org/10.1007/s11481-019-09872-z) contains supplementary material, which is available to authorized users.

✉ Catherine Huck
catherine.huck@novartis.com

[1] Autoimmunity, Transplantation and Inflammation, Novartis Institutes for Biomedical Research, Basel, Switzerland

[2] Neuroscience Development Unit, Novartis Pharma AG, Basel, Switzerland

[3] Genomics Institute of the Novartis Research Foundation, San Diego, CA, USA

to the B cell surface, inducing efficient complement-dependent cytotoxicity (CDC) and antibody-dependent cell-mediated cytotoxicity (ADCC), even when CD20 expression is low (Bar-Or et al. 2018).

In MS, treatment with rituximab and ocrelizumab is based on i.v. dosing, typically 300–1000 mg per infusion (Du et al. 2017). In contrast, ofatumumab is a subcutaneous therapy administered at 20 mg per injection (Bar-Or et al. 2018). The impact of s.c. dosing of anti-CD20 therapies on B cell subsets in major B cell compartments is largely unknown. To bridge this gap, we explored the B cell depleting capacity of a low-dose s.c. mouse anti-CD20 antibody in blood, the spleen and lymph nodes from a) healthy mice; b) mice following immune activation via two different models, the first which induces thymus-independent responses (trinitrophenylated-lipopolysaccharide [TNP-LPS]) and the second induces thymus-dependent responses (dinitrophenyl-keyhole limpet hemocyanin [DNP-KLH]); and c) mice studied in a chronic neuroinflammation experimental autoimmune encephalomyelitis (EAE) model. Immuno-phenotyping was complemented by quantitating CD20 protein expression on B cell subpopulations.

Methods

Animal Preparation and Antibody Treatment

Female C57BL/6 (9–10 weeks old) and BALB/c (9–10 weeks old) mice were commercially purchased from Envigo (Envigo RMS GmbH, Venray, AN the Netherlands). All animal work was performed in accordance with protocols approved by the Cantonal Veterinary Office of Basel-Stadt and the regulations defined by the European Community Council Directive for animal protection. Mice were specific pathogen free and maintained within individually ventilated cages with a 12/12 h light/dark cycle.

Monoclonal anti-mouse CD20 antibody (clone 18B12, IgG2a) (Ahuja et al. 2007; Moritoki et al. 2009; Yu et al. 2008) in phosphate-buffered saline (PBS) was administered subcutaneously between the iliac crest and linea alba. An isotype (MOPC-173, Bio Legend, San Diego, CA, USA) was used as a control.

On Day 0, naïve C57BL/6 mice were administered with low-dose (20 μg/mouse) s.c. anti-mouse CD20 antibody. The control group received a single dose of the respective isotype control subcutaneously. Treatment-induced changes in B cell populations were characterized in blood, axillary lymph nodes and the spleen at 19.2 h and at Days 1, 2, 3, 7, 14, 21, 28, 35 and 42 after administration via flow cytometry. Four untreated mice were used as controls.

Immune Activation Via Two Mouse Models

Trinitrophenylated Lipopolysaccharide (TNP-LPS) Immunization

The 2,4,6-trinitrophenyl-lipopolysaccharide (TNP-LPS, Sigma-Aldrich Corporation, St Louis, MO, USA) was dissolved in PBS. In order to induce thymus-independent responses, 1.5 mg/kg TNP-LPS was injected intravenously (tail vein) at Day 0.

Dinitrophenyl-Keyhole Limpet Hemocyanin (DNP-KLH) Immunization

Keyhole limpet hemocyanin (KLH; Merck KGaA, Darmstadt, Germany) conjugated to 2,4-Dinitrophenyl (DNP; Sigma-Aldrich Corporation, St Louis, MO, USA) was prepared, at a ratio of 1:20, as DNP-KLH stock solution (5 mg/mL). In order to induce thymus-dependent responses, DNP-KLH was adsorbed onto colloidal aluminum hydroxide (Alu-Gel-S, SERVA Electrophoresis GmbH, Heidelberg, Germany: 1 mL, DNP-KLH: 5 mL, PBS: 4 mL) and was injected intraperitoneally (i.p.) into BALB/c mice at 5 mg/kg.

In both these immunization models, 20 μg of anti-CD20 antibody was administered subcutaneously. The control group received a single dose of the respective isotype control subcutaneously. The antibody was administered 3 days prior to immunization and 4 days post-immunization (Figs. 4a and 6a). Serum was collected at study termination to assess DNP-/TNP- specific immunoglobulin levels. Axillary lymph nodes, the spleen and blood were investigated for B cell subsets using flow cytometry.

Induction and Assessment of EAE

Female C57BL/6 mice were immunized as described previously (Hjelmstrom et al. 1998; Oliver et al. 2003). Briefly, mice were administered with a s.c. injection of recombinant human myelin oligodendrocyte glycoprotein (MOG) peptide (in-house produced human MOG1–125; 200 μg/100 μL) emulsified in 4 mg/mL complete Freund's adjuvant (Sigma-Aldrich Corporation, St Louis, MO,) on the lower back. Mice were administered with pertussis toxin (Sigma-Aldrich; 200 ng per mouse) i.p. at Day 0 and Day 2. The disease was monitored daily using a scoring system (0: normal appearance; 1: complete tail paralysis; 2: unilateral partial hind limb paralysis; 3: complete bilateral hind limb paralysis; 4: quadriplegia; 5: death).

CD20 Protein Frequency on B Cell Subpopulations

The frequency of CD20 molecules per B cell was established by using the Quantibrite PE kit (BD

Biosciences, Franklin Lakes, NJ, USA). Five thousand events were observed on an LSR FORTESSA flow cytometer. Data were analyzed using the FlowJo software (Flow Jo LLC, Ashland, OR, USA). The flow cytometry methodology is detailed in the supplementary methods.

Enzyme-Linked Immunosorbent Assay for Serum Immunoglobulin G and Immunoglobulin M Concentrations

The presence of vaccination antigen-specific immunoglobulin (Ig) G- or IgM antibodies in serum was determined using an in-house sandwich enzyme linked immunosorbent assay (ELISA). Details of this methodology are included in the supplementary methods.

Statistical Analysis

A parametric unpaired Student's t test was used to analyze the flow cytometry and ELISA data. EAE disease scores were analyzed using non parametric Mann-Whitney rank sum tests. All analyses were performed using GraphPad Prism (version 4.00; GraphPad Software, San Diego, California, USA), and a value of $p < 0.05$ was considered significant.

Results

Rapid B Cell Depletion and Repletion in Blood, Axillary Lymph Nodes and the Spleen

Quantification of B cell frequency following a single administration of the anti-CD20 treatment in healthy mice revealed the highest depletion in blood followed by lymph nodes and the spleen (Fig. 1a–c). Repletion kinetics was rapid with around 80% recovery within 21 days of treatment cessation (Fig. 1).

In the spleen of healthy mice ($n = 3$–4 mice per time point), the absolute frequency of marginal zone (MZ) B cells decreased within 7 days of anti-CD20 treatment (Fig. 2a); however, this subset of B cells also recovered rapidly post treatment, resulting in normalized levels prior to Day 28. Although the treatment led to a depletion of MZ B cells, this subset was relatively spared as evidenced by the increase in the proportion of MZ B cells to the total B cells from 4.8% to 28.6% on Day 7 when compared to the isotype control. The proportion of MZ B cells to the total number of B cells remained high until Day 21. Follicular (FO) B cells demonstrated a distinct pattern of depletion and repletion. Maximal depletion on Day 7 was much more pronounced than the depletion observed for MZ B cells; moreover, the proportion of follicular B cells within the total B cell pool went down on Day 7 (from 78% to 24%) while the proportion of MZ B cells went up. There was a rapid repletion to normalized levels by Day 28 (Fig. 2b). The germinal center (GC) B cells remained depleted up to Day 21 (Fig. 2c), however the repletion was rapid with the absolute frequency of GC B cells being at least equivalent to the isotype control beyond Day 28. Similar to the MZ B cells, the study treatment also had a sparing effect on the GC B cells, as evidenced by their ratio to the total B cells on Day 7 (Fig. 2c).

The FO B Cell Subset Is Relatively Resistant to Low-Dose s.c. Anti-CD20 Treatment

In the axillary lymph nodes of healthy mice, anti-CD20 treatment resulted in rapid MZ B cell depletion with subsequent repletion within 21 days following treatment cessation (Fig. 3a). Similar to the findings in the spleen, the sparing

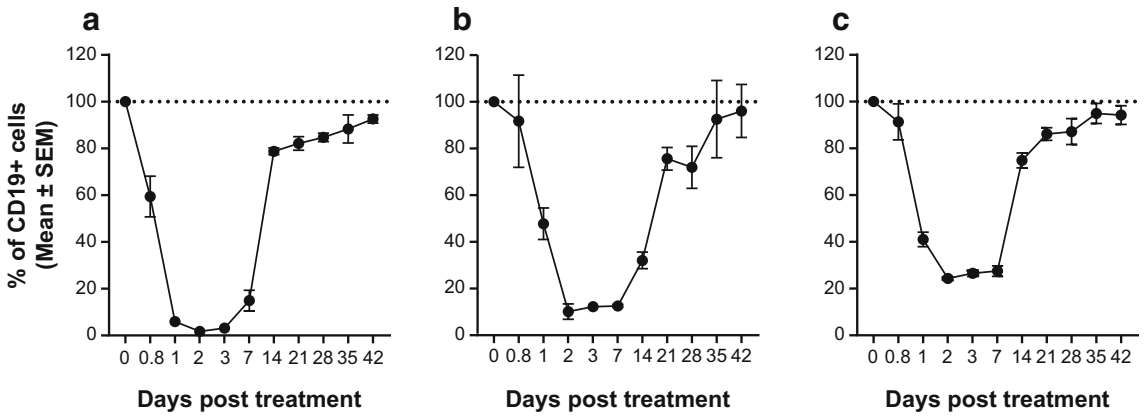

Fig. 1 B cell depletion and repletion in (a) blood, (b) axillary lymph nodes and (c) spleen, following single s.c. administration of the anti-CD20 antibody in healthy mice. Data normalized to the isotype control (dotted line). Mean ± SEM represented, $n = 3$–6 mice per group. CD, cluster of differentiation; s.c., subcutaneous; SEM, standard error of mean

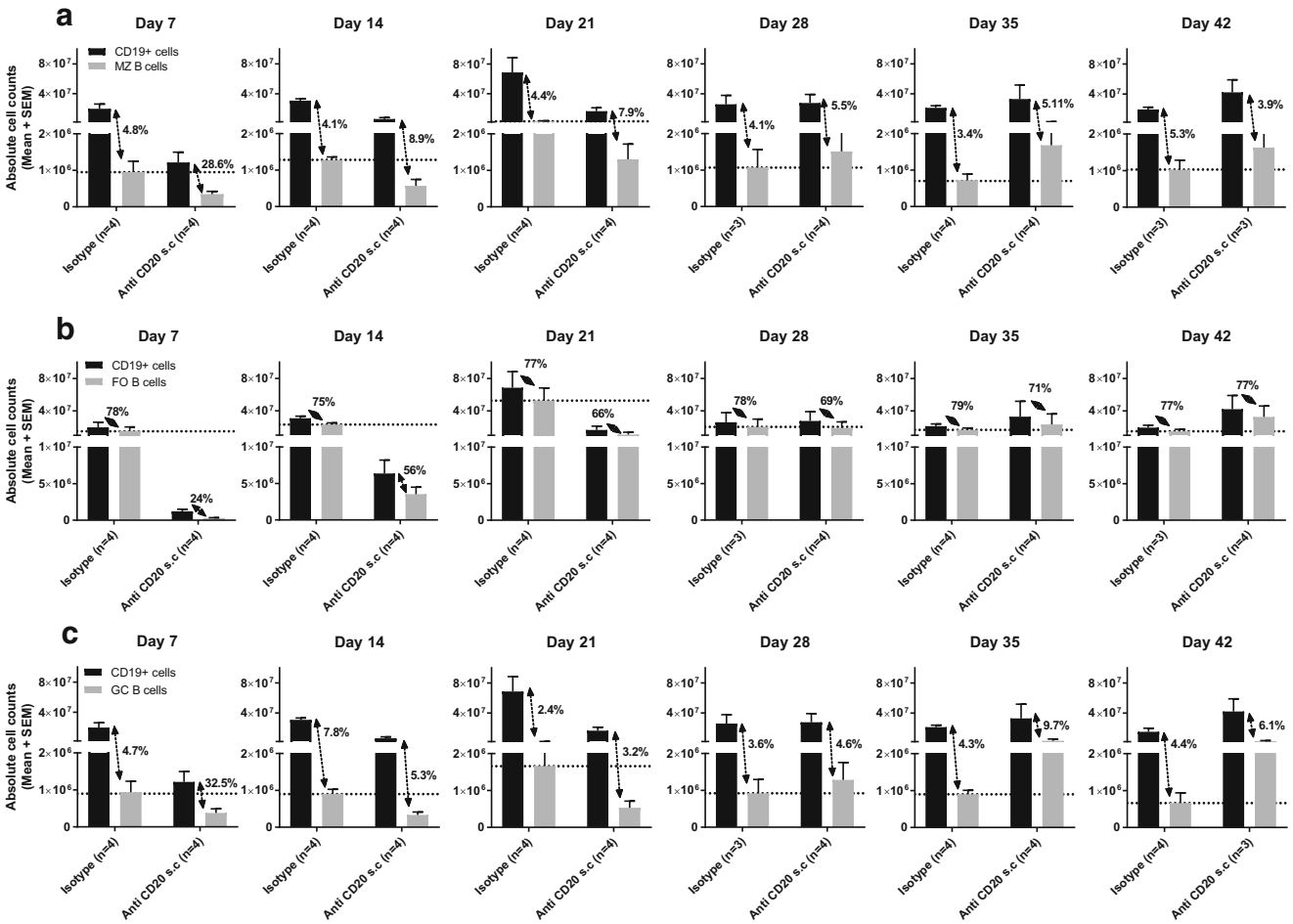

Fig. 2 Splenic B cell subset quantification of (a) marginal zone, (b) follicular and (c) germinal center subsets following single s.c. administration of the anti-CD20 antibody in healthy mice. Percentage values are the subset proportions within the total CD19+ population. Data benchmarked to the post treatment isotype control (dotted line). Mean ± SEM represented, $n = 5–6$ mice per group. CD, cluster of differentiation; FO, follicular; GC, germinal center; MZ, marginal zone; s.c., subcutaneous; SEM, standard error of mean

effect on MZ B cells was also evident in the lymph nodes, where s.c. anti-CD20 dosing led to a relative increase in MZ B cells (i.e. from 1.9% to 27.0% of the overall B cell population at Day 7). The FO B cells in the lymph nodes were potently depleted by the anti-CD20 treatment with the lowest levels observed on Day 7, gradually improving over the subsequent time points and reaching normalized levels by Day 35 (Fig. 3b). As observed in the spleen, the proportion of FO B cells within the total B cells decreased, while the proportion of MZ B cells increased. In terms of lymph node GC B cells, anti-CD20 treatment led to a sustained depletion up to Day 21 followed by a recovery by Day 35 (Fig. 3c). All B cell subsets repleted to normalized levels by Day 21.

Cell Membrane CD20 Expression Varied Among B Cell Subsets in the Blood, Lymph Node (Both Axillary and Inguinal) and the Spleen

In blood, CD20 protein was expressed consistently on all B cell subsets (Supplemental Fig. 1a). In contrast, within axillary and inguinal lymph nodes, CD20 expression was more pronounced in the GC B cells compared to FO and MZ populations (Supplemental Fig. 1b & c). Compared with B cell subsets in blood and lymph nodes, CD20 expression was higher in all splenic B cells. Furthermore, the MZ B cells in the spleen had significantly ($p < 0.01$) higher CD20 expression than the other subsets isolated from the same tissue (Supplemental Fig. 1d).

Anti-CD20 Treatment Did Not Impair TNP-LPS-Induced Immunoglobulin Responses

Anti-CD20 treatment was initiated prior to TNP-LPS i.v. immunization (Fig. 4a), which triggered a T cell independent B cell immune response in the form of antigen-specific antibody production. Analysis of TNP-specific IgM and IgG revealed that low-dose anti CD20 treatment did not impair humoral response to antigenic stimuli (Fig. 4b and c). Both IgM and IgG titers were significantly higher with the anti-CD20 antibody versus the isotype control.

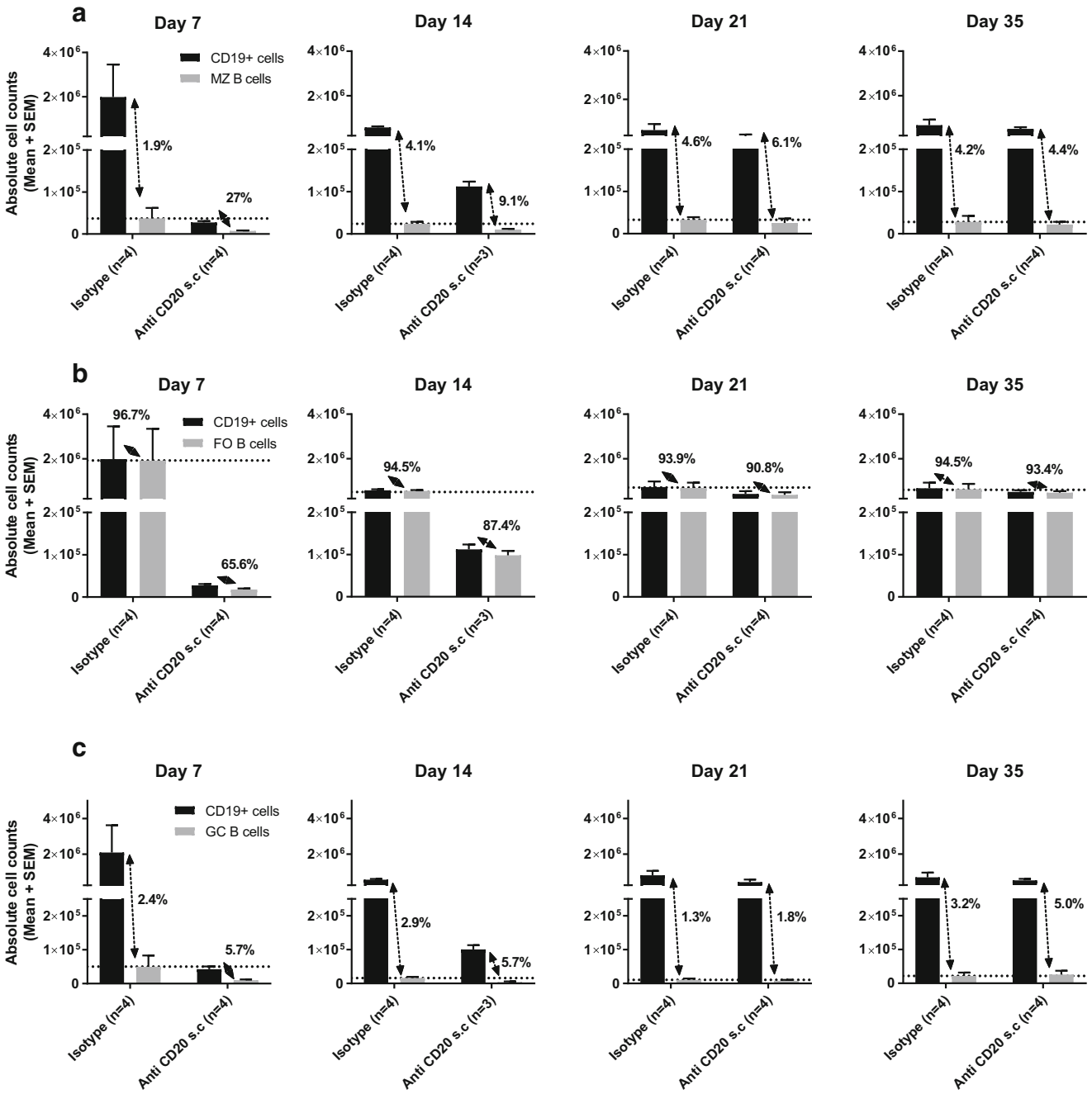

Fig. 3 Axillary lymph node B-cell subset quantification of (a) marginal zone, (b) follicular and (c) germinal center subsets following single s.c. administration of the anti-CD20 antibody in healthy mice. Percentage values are the subset proportions within the total CD19+ population. Data benchmarked to the post treatment isotype control (dotted line). Mean ± SEM represented, $n = 5–6$ mice per group. CD, cluster of differentiation; FO, follicular; GC, germinal center; MZ, marginal zone; s.c., subcutaneous; SEM, standard error of mean

The Anti-CD20-Mediated B Cell Subset Depletion Profile Is Consistent Between Quiescent and Immune Activation

Analysis of B cell subsets within the spleen and inguinal lymph nodes of TNP-LPS-immunized mice revealed that all the B cell subsets were depleted in both tissue samples (Fig. 5a to f). Compared to the isotype control, anti-CD20 treatment led to relative sparing of MZ B cells in both tissue samples with higher proportions of these cells in the spleen (2.3% vs. 12%) and inguinal lymph nodes (1% vs. 5%). A similar sparing effect was observed with GC B cells; the effect was more prominent in the inguinal lymph nodes (4.4% vs. 36.2%) than in the spleen (1.7% vs. 7.8%).

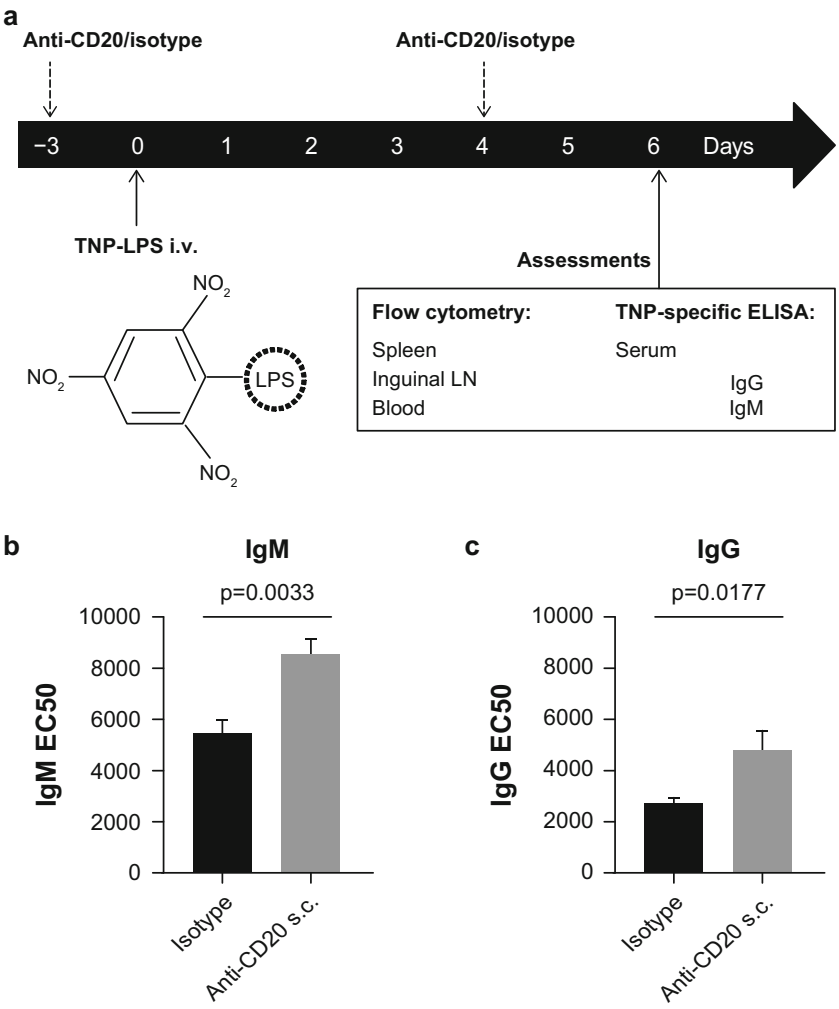

Fig. 4 Anti-CD20 treatment in (a) TNP-LPS did not impair T cell independent TNP-LPS-mediated **TNP-specific (b) IgM and (c) IgG antibody formation.** Mean + SEM represented, $n = 4$ animals per group. CD, cluster of differentiation; EC50, concentration of a drug that gives half-maximal response; ELISA, enzyme linked immunosorbent assay; Ig, immunoglobulin; i.v., intravenous; LN, lymph node; s.c., subcutaneous; SEM, standard error of mean; TNP-LPS, trinitrophenylated lipopolysaccharide

No sparing effect was observed in the case of FO B cells, on the contrary, the relative proportion of follicular B cells within the total B cells went down.

Enhanced T Cell Dependent IgM Response Following Low-Dose s.c. Anti-CD20 Therapy

Anti-CD20 treatment was initiated prior to DNP-KLH intraperitoneal immunization (Fig. 6a), which triggered a T cell dependent B cell antigen (DNP)-specific immune response. Low-dose s.c. treatment significantly enhanced antigen-specific IgM responses but IgG switching was unchanged when compared with the isotype controls (Fig. 6b and c).

Low-Dose s.c. Anti-CD20 Treatment Relatively Spared MZ B Cells During a T Cell Dependent B Cell Immunization Model

Quantification of absolute B cell subset frequencies following DNP-KLH immunization in the spleen and inguinal lymph nodes revealed higher depletion in the FO B cells than in MZ and GC B cells in both tissue samples (Fig. 7a–f). Compared to the isotype control, anti-CD20 treatment led to sparing of MZ B cells in both tissue samples with higher proportions of these cells in the spleen (0.16% vs. 0.4%) and inguinal lymph nodes (1% vs. 1.5%). Similar to the TNP-LPS model, the sparing effect on GC B cells was more prominent in the inguinal lymph nodes (5.9% vs. 37%) than in the spleen (4.4% vs. 20.6%). No sparing effect was observed in the case of FO B cells.

Low-Dose s.c. Anti-CD20 Inhibited Neuroinflammation Severity

Human MOG protein-induced EAE requires B cells for (auto) antigen presentation to generate pathogenic T-cells (Hjelmstrom et al. 1998; Oliver et al. 2003). Short-term prophylactic low-dose s.c. treatment resulted in significantly lower EAE score (both daily and cumulative) when compared

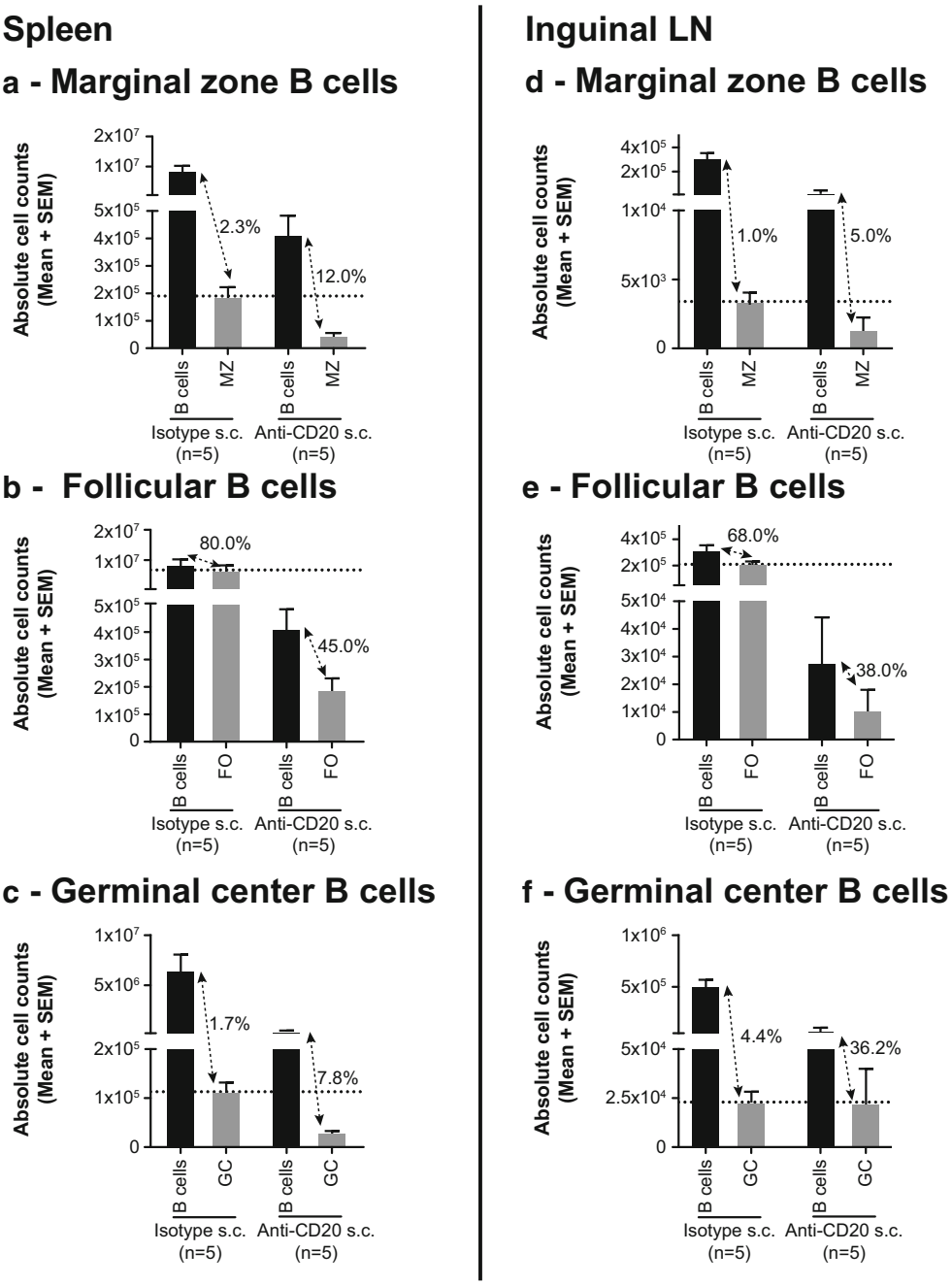

Fig. 5 Spleen tissue resident B cells are differentially sensitive to anti-CD20 treatment regimens during a T cell independent immune response as shown splenic (a) marginal zone, (b) follicular and (c) germinal center B-cell subpopulations and lymph node (d) marginal zone, (e) follicular and (f) germinal center B-cell subpopulations. Mean + SEM represented, $n = 4$ animals per group. CD, cluster of differentiation; FO, follicular; GC, germinal center; LN, lymph node; MZ, marginal zone; s.c., subcutaneous; SEM, standard error of mean; TNP-LPS, trinitrophenylated lipopolysaccharide

with the isotype solution, suggesting a decreased disease burden (Fig. 8a and b).

Low-Dose Subcutaneous Anti-CD20 Therapy Depletion Effectively Targeted the Neuroinflammation Relevant B Cells in Lymphoid Tissues

Analysis of immune compartments during anti-CD20-modulated autoimmune neuroinflammation showed that the maximal B cell depletion was achieved within 2 days of treatment and it was highest in the lymph nodes (Fig. 8c–e). Regardless of the tissues analyzed, low-dose s.c. treatment was characterized by a rapid B cell repletion following anti-CD20 treatment cessation (Fig. 8c–e).

Discussion

Depletion of B cells by anti-CD20 mAb therapy has been proven efficacious in multiple autoimmune diseases such as MS (Edwards and Cambridge 2001; Stone et al. 2010;

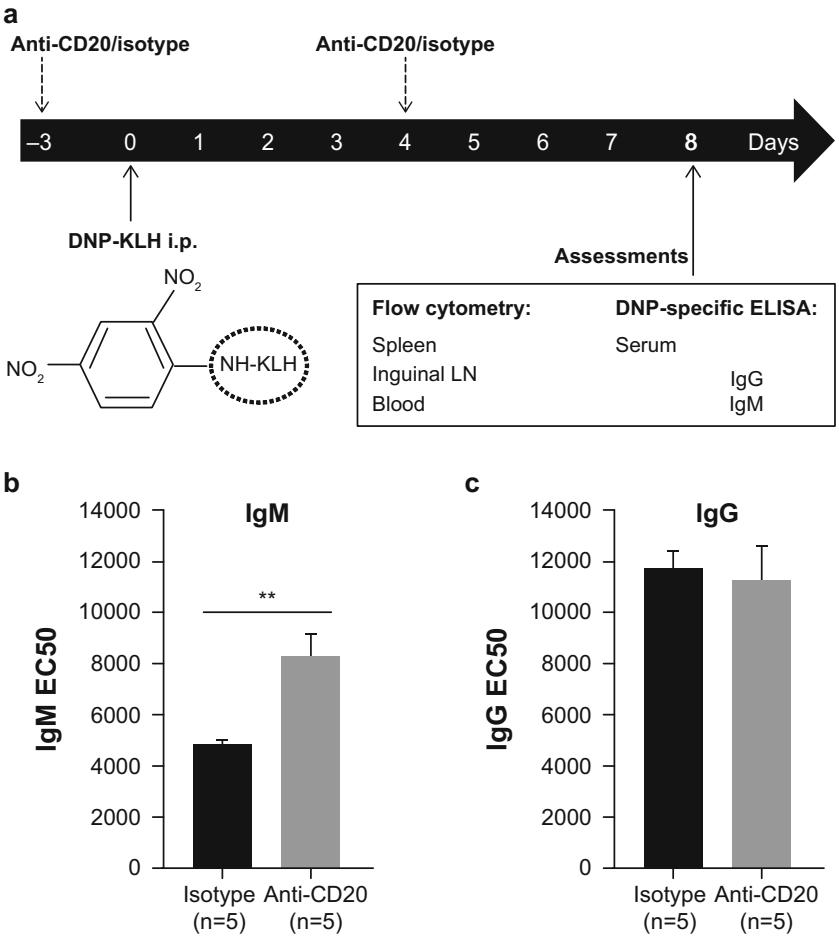

Fig. 6 Low-dose anti-CD20 treatment in (a) DNP-KLH model does not negatively impact T cell dependent DNP-specific (b) IgM and (c) IgG antibody formation. Mean + SEM represented, $n = 4$ animals per group. CD, cluster of differentiation; DNP-KLH, dinitrophenyl-keyhole limpet hemocyanin; ELISA, enzyme linked immunosorbent assay; Ig, immunoglobulin; LN, lymph node; s.c., subcutaneous; SEM, standard error of mean

Turner-Stokes et al. 2011). The treatment regimens of anti-CD20 mAbs administered at high dose intravenously in MS patients have been directly derived from oncology trials (McLaughlin et al. 1998; Morschhauser et al. 2010). By contrast, in the MIRROR trial and the ongoing Phase III trials, ofatumumab is administered at a low dose subcutaneously. (Bar-Or et al. 2018; Kappos et al. 2018) In the current study, we have mimicked a low-dose s.c. human dosing regimen of anti-CD20 therapy in a healthy and immuno-modulated mice to better understand the extent to which B cell subsets are affected in blood and lymphoid organs.

In healthy mice, a comparable B cell maximal depletion was observed in blood and lymph nodes, however splenic B cells demonstrated a delayed maximal depletion. Overall, B cells were depleted very rapidly (i.e. within the first 2 days of treatment) with swift repletion kinetics of ~80% recovery within 21 days of treatment cessation.

The s.c. anti-CD20 treatment relatively spared MZ B cells in the spleen of healthy mice as well as in the spleen and lymph nodes of the TNP-LPS mouse model. Moreover, the s.c. anti-CD20 mAb therapy did not impair the production of TNP-specific IgM and IgG antibodies. The trinitrophenylated derivatives of lipopolysaccharide (TNP-LPS) elicit a specific anti-TNP, thymus-independent immune response, which mimic blood-borne bacterial stimuli (Humbert et al. 1979). MZ B cells, an important subset as the first-line defense against systemic blood-borne infections, are mainly involved in rapid innate immune responses (Cerutti et al. 2013). Our results indicate that low-dose s.c. anti-CD20 therapy may preserve to a certain extent important immune surveillance mechanisms against blood-borne pathogens.

The DNP-KLH model mimics a vaccination acute response (the first stage of developing immunological memory) with a T cell dependent B cell immune response requiring GC formation for antibody production (Hauser et al. 2017). We found that s.c. anti-CD20 therapy resulted in some sparing of MZ B cells and GC B cells in this model. Furthermore, the s.c. anti-CD20 treatment significantly enhanced antigen-

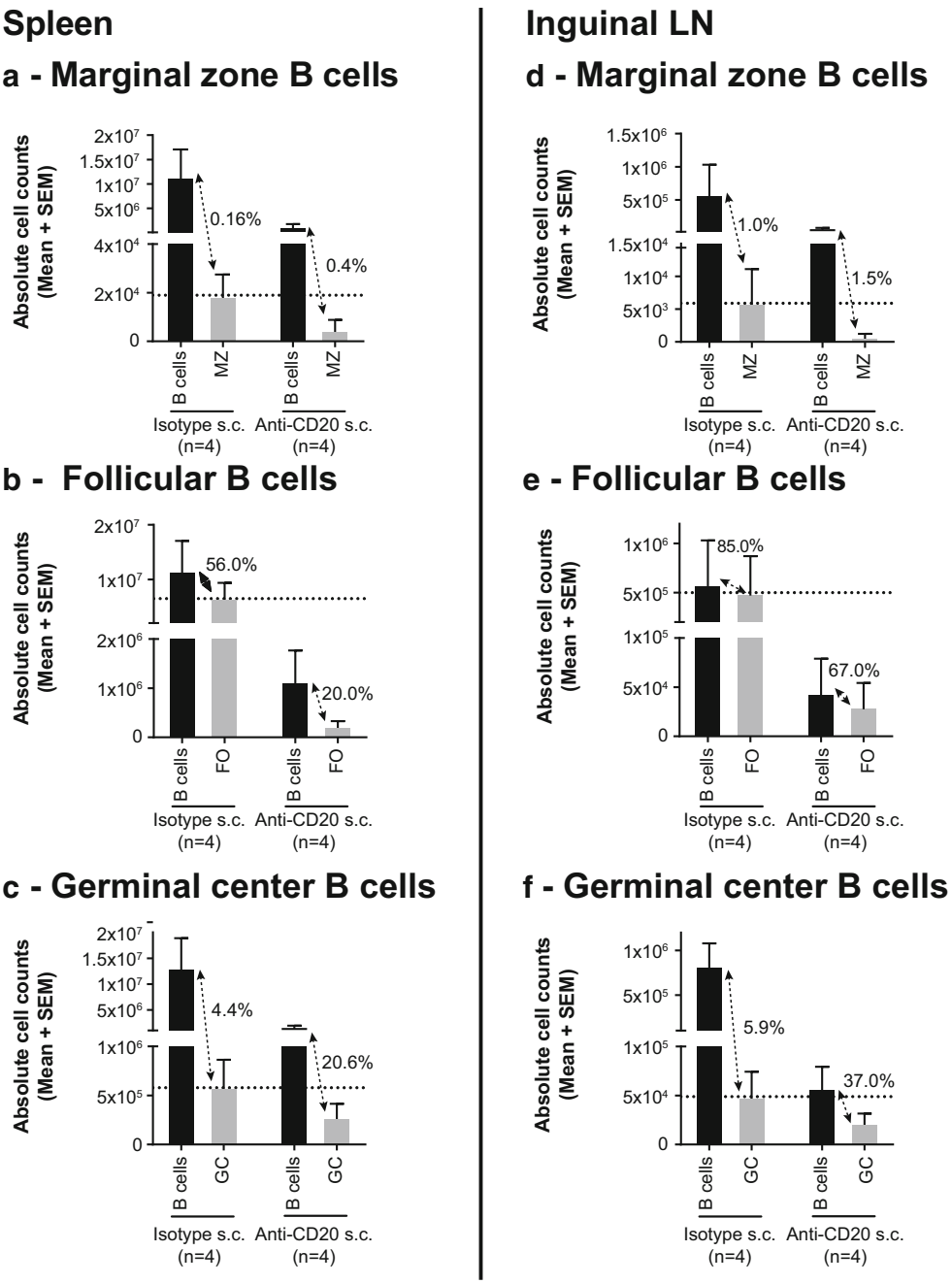

Fig. 7 Effects of anti-CD20 therapy on (a, d) marginal zone, (b, e) follicular and (c, f) germinal center B-cell subsets within the spleen and lymph node tissues respectively during a thymus-dependent immune response in mice. Mean + SEM represented, $n = 4$ animals per group. CD, cluster of differentiation; DNP-KLH, dinitrophenyl-keyhole limpet hemocyanin; FO, follicular; GC, germinal center; LN, lymph node; MZ, marginal zone; s.c., subcutaneous; SEM, standard error of mean

specific IgM responses, suggesting that the s.c. dosing regimen does not hinder the immune function in a primary vaccination response.

In the EAE model, low-dose s.c. anti-CD20 therapy effectively targeted disease-relevant B cell populations within lymphatic tissues and was effective in reducing central nervous system autoimmunity. This may be attributed to the facilitation of macromolecule absorption via lymphatic capillaries (Ali Khan et al. 2013). Migotto et al. demonstrated that the s.c. mouse anti-CD20 antibody is preferentially distributed to the lymph nodes and blood, and to a lesser extent to the spleen, compared to the distribution following i.v. administration (Migotto et al. 2018).

In the present study, maximal B cell depletion and subset sensitivity to anti-CD20 therapy appeared similar in healthy, immunized and autoimmune disease settings, suggesting that B cell susceptibility to CDC and ADCC as the basis for the observed B cell depletion in mouse

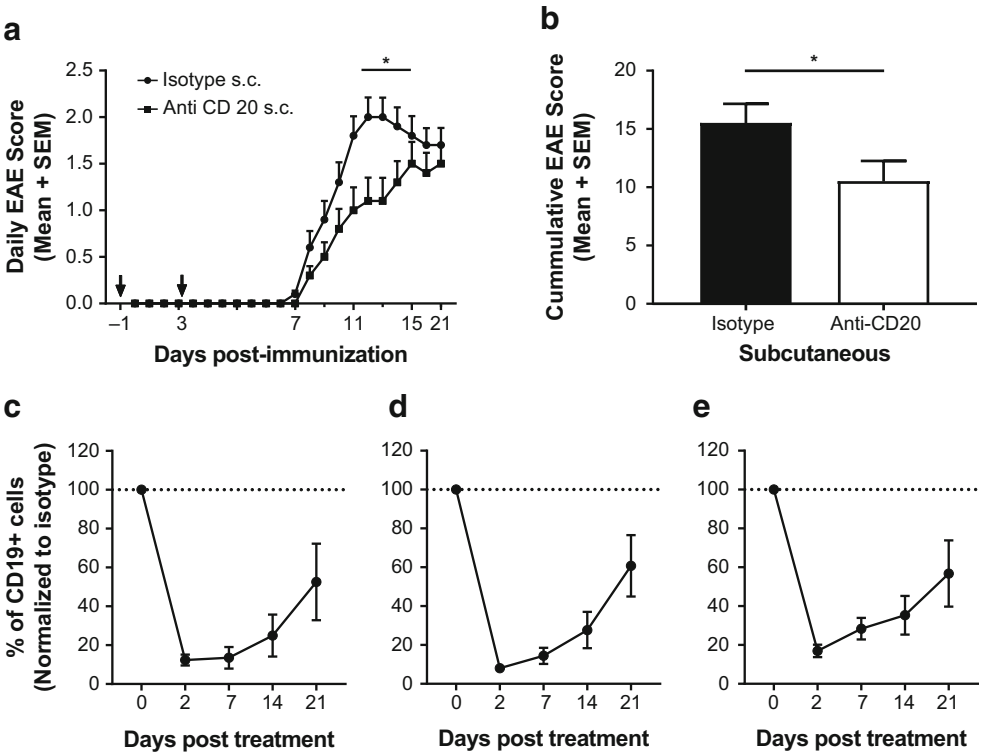

Fig. 8 Neurological score/ disease burden and B-cell quantification following s.c. anti-CD20 treatment in a mouse EAE pilot study using human MOG peptide (MOG1–125). a Daily neurological score and (b) total disease burden, and percentage of CD19+ B cells following s.c. anti-CD20 treatment in (c) blood, (d) inguinal lymph nodes and (e) the spleen. Dosing indicated by black arrows. Mean + SEM represented, $n = 8$–24 animals per group in **a** and **b**. Mean ± SEM represented, $n = 4$ animals per group in **c**, *d* and **e**. $^{*}p < 0.05$; $^{**}p < 0.01$. CD, cluster of differentiation; EAE, experimental autoimmune encephalomyelitis; iso, isotype; MOG, myelin oligodendrocyte glycoprotein; s.c., subcutaneous; SEM, standard error of mean

blood and tissue remains consistent regardless of immune activation state. Our study also demonstrated rapid repletion of B cells following treatment cessation. This may represent an advantage in patients with an increased risk of opportunistic infections who may need to be off-drug quickly. The ongoing clinical trials with ofatumumab will be instrumental in assessing the clinical relevance of our observations.

The absolute CD20 protein expression per cell varies between B cell subsets, which potentially alters the relative susceptibility to antibody-mediated depletion and has been described for rituximab and ofatumumab (Leandro 2013). The phenomena of low CD20 B cell lymphomas evading rituximab-mediated chemotherapy is well described (Tomita 2016). We observed that, although CD20 expression of all B cell subsets was higher in the spleen with MZ B cells being significantly higher than other B cell subsets, it did not have much impact on the effect of low dose s.c. therapy on these B cell subsets in healthy mice.

In summary, disease-relevant B cell populations within lymphatic tissues were effectively targeted by low-dose s.c. anti-CD20 therapy, which reduced the severity of neuroinflammation. These data suggest that s.c. anti-CD20 therapies can effectively target disease-relevant B cell populations while improving repletion kinetics and maintaining vaccination responses, thereby achieving autoimmune amelioration without severely impacting immune surveillance functions.

Acknowledgments This study was funded by Novartis Pharma AG. The authors would like to acknowledge the laboratory animal services technical team for in vivo support. The authors would like to thank Richa Chhabra and Sivaram Vedantam (Medical communications, Novartis Healthcare Pvt. Ltd) for medical writing assistance in developing the first draft of the manuscript, formatting, referencing and incorporating the authors' revisions and submission, all under the direction of the authors.

Authors' Contributions PAS and CH designed the studies, interpreted the data and drafted the manuscript. VW, CS and RD contributed experimental data. GW contributed to experimental designs, data evaluation and writing the manuscript. DL contributed to experimental designs and data evaluation. All authors have read and approved the final manuscript.

Data Availability The datasets generated and/or analyzed during the current study are available from the corresponding author on reasonable request.

Compliance with Ethical Standards

Animal Ethics Statement All animal work was performed according to the Swiss federal law for animal protection and approved by the Veterinary Office of the Canton Basel-Stadt.

Conflict of Interest Catherine Huck, Cindy Schmid, Robert Dunn and Gisbert Weckbecker are employees of Novartis Pharma AG, Basel, Switzerland.

Paul Smith, David Leppert and Vanessa Wegert were employed by Novartis Pharma AG, Basel, Switzerland during the conduct of the study.

References

Ahuja A, Shupe J, Dunn R, Kashgarian M, Kehry MR, Shlomchik MJ (2007) Depletion of B cells in murine lupus: efficacy and resistance. J Immunol 179(5):3351–3361. https://doi.org/10.4049/jimmunol.179.5.3351

Ali Khan A, Mudassir J, Mohtar N, Darwis Y (2013) Advanced drug delivery to the lymphatic system: lipid-based nanoformulations. Int J Nanomedicine 8:2733–2744. https://doi.org/10.2147/IJN.S41521

Bar-Or A, Calabresi PA, Arnold D, Markowitz C, Shafer S, Kasper LH, Waubant E, Gazda S, Fox RJ, Panzara M, Sarkar N, Agarwal S, Smith CH (2008) Rituximab in relapsing-remitting multiple sclerosis: a 72-week, open-label, phase I trial. Ann Neurol 63(3):395–400. https://doi.org/10.1002/ana.21363

Bar-Or A, Grove RA, Austin DJ, Tolson JM, VanMeter SA, Lewis EW, Derosier FJ, Lopez MC, Kavanagh ST, Miller AE, Sorensen PS (2018) Subcutaneous ofatumumab in patients with relapsing-remitting multiple sclerosis: the MIRROR study. Neurology 90(20):e1805–e1814. https://doi.org/10.1212/WNL.0000000000005516

Cerutti A, Cols M, Puga I (2013) Marginal zone B cells: virtues of innate-like antibody-producing lymphocytes. Nat Rev Immunol 13(2):118–132. https://doi.org/10.1038/nri3383

Du FH, Mills EA, Mao-Draayer Y (2017) Next-generation anti-CD20 monoclonal antibodies in autoimmune disease treatment. Auto Immun Highlights 8(1):12. https://doi.org/10.1007/s13317-017-0100-y

Edwards JC, Cambridge G (2001) Sustained improvement in rheumatoid arthritis following a protocol designed to deplete B lymphocytes. Rheumatology (Oxford) 40(2):205–211

Gong Q, Ou Q, Ye S, Lee WP, Cornelius J, Diehl L, Lin WY, Hu Z, Lu Y, Chen Y, Wu Y, Meng YG, Gribling P, Lin Z, Nguyen K, Tran T, Zhang Y, Rosen H, Martin F, Chan AC (2005) Importance of cellular microenvironment and circulatory dynamics in B cell immunotherapy. J Immunol 174(2):817–826

Gorman C, Leandro M, Isenberg D (2003) B cell depletion in autoimmune disease. Arthritis Res Ther 5(Suppl 4):S17–S21. https://doi.org/10.1186/ar1007

Hauser SL, Waubant E, Arnold DL, Vollmer T, Antel J, Fox RJ, Bar-Or A, Panzara M, Sarkar N, Agarwal S, Langer-Gould A, Smith CH, Group HT (2008) B-cell depletion with rituximab in relapsing-remitting multiple sclerosis. N Engl J Med 358(7):676–688. https://doi.org/10.1056/NEJMoa0706383

Hauser SL, Bar-Or A, Cohen J, Comi G, Correale J, Coyle PK et al (2017) Ofatumumab versus teriflunomide in relapsing MS: adaptive design of two phase 3 studies (ASCLEPIOS I and ASCLEPIOS II)(S16. 005). Neurology 88(16 Supplement):S16. 005

Hjelmstrom P, Juedes AE, Fjell J, Ruddle NH (1998) B-cell-deficient mice develop experimental allergic encephalomyelitis with demyelination after myelin oligodendrocyte glycoprotein sensitization. J Immunol 161(9):4480–4483

Humbert J, Motta I, Truffa-Bachi P (1979) TNP-LPS induces an IgG anti-TNP immune response in mice. Cell Immunol 47(1):211–217

Kappos L, Bar-Or A, Cohen J, Comi G, Correale J, Coyle PK, Cross AH, De Seze J, Montalban X, Selmaj K, Wiendl H, Kerloeguen C, Willi R, Haring DA, Leppert D, Goodyear A, Tomic D, Kakarieka A, Hauser S (2018) Ofatumumab versus teriflunomide in relapsing multiple sclerosis: baseline characteristics of two pivotal phase 3 trials (ASCLEPIOS I and ASCLEPIOS II). Mult Scler J 24:526–527

Leandro MJ (2013) B-cell subpopulations in humans and their differential susceptibility to depletion with anti-CD20 monoclonal antibodies. Arthritis Res Ther 15(Suppl 1):S3. https://doi.org/10.1186/ar3908

Lemus HN, Warrington AE, Rodriguez M (2018) Multiple Sclerosis: mechanisms of disease and strategies for myelin and axonal repair. Neurol Clin 36(1):1–11. https://doi.org/10.1016/j.ncl.2017.08.002

McLaughlin P, Grillo-Lopez AJ, Link BK, Levy R, Czuczman MS, Williams ME, Heyman MR, Bence-Bruckler I, White CA, Cabanillas F, Jain V, Ho AD, Lister J, Wey K, Shen D, Dallaire BK (1998) Rituximab chimeric anti-CD20 monoclonal antibody therapy for relapsed indolent lymphoma: half of patients respond to a four-dose treatment program. J Clin Oncol 16(8):2825–2833. https://doi.org/10.1200/JCO.1998.16.8.2825

Migotto MA, Bhalla R, Mardon K, Orian J, Weckbecker G, Kneuer R et al (2018) Imaging and biodistribution of a novel anti-CD20 antibody following SubcutaneousAdministration in control and experimental autoimmune encephalomyelitis-variant mice. Mult Scler 2018; 24: (S2) 530–737 (P1066)

Moritoki Y, Lian ZX, Lindor K, Tuscano J, Tsuneyama K, Zhang W, Ueno Y, Dunn R, Kehry M, Coppel RL, Mackay IR, Gershwin ME (2009) B-cell depletion with anti-CD20 ameliorates autoimmune cholangitis but exacerbates colitis in transforming growth factor-beta receptor II dominant negative mice. Hepatology 50(6):1893–1903. https://doi.org/10.1002/hep.23238

Morschhauser F, Marlton P, Vitolo U, Linden O, Seymour JF, Crump M, Coiffier B, Foa R, Wassner E, Burger HU, Brennan B, Mendila M (2010) Results of a phase I/II study of ocrelizumab, a fully humanized anti-CD20 mAb, in patients with relapsed/refractory follicular lymphoma. Ann Oncol 21(9):1870–1876. https://doi.org/10.1093/annonc/mdq027

Mulero P, Midaglia L, Montalban X (2018) Ocrelizumab: a new milestone in multiple sclerosis therapy. Ther Adv Neurol Disord 11:1756286418773025. https://doi.org/10.1177/1756286418773025

Oliver AR, Lyon GM, Ruddle NH (2003) Rat and human myelin oligodendrocyte glycoproteins induce experimental autoimmune encephalomyelitis by different mechanisms in C57BL/6 mice. J Immunol 171(1):462–468. https://doi.org/10.4049/jimmunol.171.1.462

Stone JH, Merkel PA, Spiera R, Seo P, Langford CA, Hoffman GS, Kallenberg CG, St Clair EW, Turkiewicz A, Tchao NK, Webber L, Ding L, Sejismundo LP, Mieras K, Weitzenkamp D, Ikle D, Seyfert-Margolis V, Mueller M, Brunetta P, Allen NB, Fervenza FC, Geetha D, Keogh KA, Kissin EY, Monach PA, Peikert T, Stegeman C, Ytterberg SR, Specks U, Group R-IR (2010) Rituximab versus cyclophosphamide for ANCA-associated vasculitis. N Engl J Med 363(3):221–232. https://doi.org/10.1056/NEJMoa0909905

Tomita A (2016) Genetic and epigenetic modulation of CD20 expression in B-cell malignancies: molecular mechanisms and significance to rituximab resistance. J Clin Exp Hematop 56(2):89–99. https://doi.org/10.3960/jslrt.56.89

Turner-Stokes T, Lu TY, Ehrenstein MR, Giles I, Rahman A, Isenberg DA (2011) The efficacy of repeated treatment with B-cell depletion therapy in systemic lupus erythematosus: an evaluation. Rheumatology (Oxford) 50(8):1401–1408. https://doi.org/10.1093/rheumatology/ker018

Yu S, Dunn R, Kehry MR, Braley-Mullen H (2008) B cell depletion inhibits spontaneous autoimmune thyroiditis in NOD.H-2h4 mice. J Immunol 180(11):7706–7713